JOURNAL OF COLLOID AND INTERFACE SCIENCE 177, 122–131 (1996)
Article No. 0012

Surface Complexation at the TiO_2 (anatase)/Aqueous Solution Interface: Chemisorption of Catechol

RAUL RODRÍGUEZ, MIGUEL A. BLESA, AND ALBERTO E. REGAZZONI[1]

Departamento Química de Reactores, Comisión Nacional de Energía Atómica, Av. del Libertador 8250, 1429-Buenos Aires, Argentina

Received January 3, 1995; accepted May 12, 1995

Catechol adsorbs at the TiO_2 (anatase)/aqueous solution interface forming inner-sphere surface complexes. The UV–visible differential reflectance spectrum of surface titanium–catecholate complexes presents a band centered at 420 nm which corresponds to the ligand to metal charge transfer transition within the surface complexes. At pH values below pK_{a1}, the surface excess of catechol is almost insensitive toward pH and presents a Langmuirian dependence with the concentration of uncomplexed catechol. The ratio $\Gamma_{max}:N_S$ (N_S being the measured density of available OH surface groups) indicates a prevailing 1 to 2 ligand exchange adsorption stoichiometry. In the range pH $\geq pK_{a1}$, the catechol surface excess decreases markedly with increasing pH. Formation of 1 to 1 surface complexes produces an excess of negative surface charge that is revealed by the shift of the iep to lower pH values. The reported data, which are supplemented with information on the charging behavior of TiO_2 suspended in indifferent electrolyte solutions, are interpreted in terms of the multi-site surface complexation model. In this model, two types of surface OH groups are considered: $\equiv TiOH^{1/3-}$ and $\equiv OH^{1/3+}$. Although both surface groups undergo protonation–deprotonation reactions, only $\equiv TiOH^{1/3-}$ are prone to chemisorption.

Key Words: surface complexation; chemisorption; TiO_2; anatase; catechol.

INTRODUCTION

The surface complexation concept is one of the most successful approaches to the rationalization of the colloid chemistry of metal oxides immersed in water (1–6). In this outlook, dissolved solutes interact with partially hydrated surface metal ions in a way that parallels solution chemistry. Thus, surface charge develops through the protonation–deprotonation of water molecules bound to surface metal ions, and adsorbing ligands form outer- and/or inner-sphere surface complexes (7, 8). Outer-sphere surface complexation takes place when electrostatic forces are the dominant contribution to the Gibbs adsorption energy (9–11). Formation of inner-sphere surface complexes, on the other hand, ensues when adsorption is driven chemically and involves the exchange of bound water molecules, or OH^-, for the adsorbing ligand (12–15); inner-sphere surface complexation is limited to the adsorption of complexing species. Recent spectroscopic evidence (16–18) and EXAFS (19, 20) characterization of adsorbed anions provide sound grounds for the widespread use of the surface complexation approach.

The surface sites have been customarily described as electroneutral $\equiv MeOH$ surface groups, a notation that accounts for their amphoteric nature and the ability of $\equiv Me$ to exchange ligands. In this description, however, all surface sites are assumed to be energetically equivalent; differences arising from the dissimilar coordination environments of the different crystal faces that may be exposed to the aqueous phase are lumped into overall surface equilibrium constants. The more general description that includes surface coordinated water molecules (7, 8, 21), i.e., $\equiv Me(OH)_m(OH_2)_n$, also presents this limitation. To overcome this liability, Hiemstra *et al.* (22–24) have recently proposed a multi-site protonation model in which the acidity and density of the different types of OH surface groups are dictated by the crystal structure of the exposed hydroxylated surfaces. The concepts underlying this model further imply that not every site would be prone to chemisorption, because the susceptibility of each type of OH surface group towards ligand exchange should depend on its coordination number.

Clearly, multisite complexation models should offer a more comprehensive picture of the chemisorption phenomena. In this paper we present a detailed study of the adsorption of catechol (1,2-dihydroxybenzene) at the TiO_2 (anatase)/solution interface and probe the applicability of the multisite surface complexation model to describe the adsorption of weak acids at metal oxide/aqueous solution interfaces.

The studied system was selected because catechol is a diprotic weak acid that prevails in the undissociated form over a wide pH range ($pK_{a1} = 9.2$; $pK_{a2} = 13.0$) and forms very stable complexes with aqueous Ti(IV) (25–27). In addition, TiO_2 aqueous suspensions behave as ideal systems; indeed, they have served to establish the basis of

[1] To whom correspondence should be addressed.

0021-9797/96 $12.00

various models for ionic adsorption, e.g., the site-binding model (9, 28, 29). Furthermore, dissociative water chemisorption on the prevailing crystal faces of both rutile and anatase yields two types of OH surface groups (30–33): hydroxyls bond to penta-coordinated titanium surface ions (i.e., $\equiv TiOH^{1/3-}$) and protons bond to di-coordinated oxo surface ions (i.e., $\equiv OH^{1/3+}$).

EXPERIMENTAL

Titanium dioxide, P-25 TiO_2, was from Degussa Corp. This solid was thoroughly washed by dialysis until the conductivity of the supernatant solution was the same of water, vacuum dried, and stored in a desiccator, in the dark. The BET specific surface area, determined from the N_2 adsorption isotherm at 77 K, was 51.4 $m^2\ g^{-1}$. The XRD pattern of the powder indicated that it is mainly anatase, the content of rutile being less than ca. 10%.

All other reagents were analytical grade and were used without further purification. Solutions were made using deionized water obtained from an E-pure apparatus (conductivity less than 10^{-5} S m^{-1}).

The Brønsted acid–base behavior of the P-25 TiO_2 surface was characterized following the well-known fast titration procedure. About 0.3 g of TiO_2 were suspended in 0.1 dm^3 of KCl solutions of desired concentration and titrated with 0.1 mol dm^{-3} HCl and 0.1 mol dm^{-3} KOH using a Metrohm 761 DMS Titrino and a 0.001 dm^3 burette; pH values were recorded 3 min after each addition of titrant. Comparison with blank titration curves yields the difference $(\Gamma_{H^+} - \Gamma_{OH^-})$.

Additional base adsorption experiments were performed to measure the density of OH surface groups. Weighted amounts of TiO_2 were suspended in KOH solutions of known concentration and allowed to equilibrate for 15 min. After removing the solid by filtration, the concentration of base in the supernatant solutions was determined potentiometrically. Each experiment was run in triplicate; experiments carried out at longer equilibration times yielded the same results.

To measure catechol adsorption isotherms, typically 0.8 g of TiO_2 were suspended in 0.05 dm^3 of freshly prepared catechol solutions of known concentration and the pH was adjusted to prefixed values by the addition of measured amounts of HCl or KOH. These suspensions were left to equilibrate for 30 min (sequential experiments indicated that catechol adsorption reached equilibrium within 10 min); during this period, pH remained constant within ±0.1. The solid was filtered off and the concentration of catechol in the supernatant solutions was determined spectrophotometrically at 275 nm. Catechol surface excesses were calculated by solving the mass balance of the systems; in all cases, blank experiments were performed. Dissolution during the course of the experiments was negligible; the concentration of dissolved Ti(IV)–catecholate complexes in the supernatants was always below 2×10^{-7} mol dm^{-3}, as indicated by the zero absorbance measured at 389 nm (cf. Refs. (25) and (27)).

TABLE 1
Adsorption of Hydroxyl Ions from KOH Solutions

$[OH^-]\ 10^3$ (mol dm^{-3})	$\Gamma_{OH^-}\ 10^6$ (mol m^{-2})	$[OH^-]/\Gamma_{OH^-}$ ($m^2\ dm^{-3}$)
4.58	2.19	2091
6.30	2.41	2614
9.49	2.54	3736

In selected cases, the filtered off solids were washed with water and vacuum-dried, and the UV–visible diffuse reflectance spectra of the powders were recorded in a Shimadzu UV-210A spectrometer.

All adsorption experiments were carried out under normal laboratory illumination at 298.0 ± 0.2 K in thermostated borosilicate glass vessels. In all cases, O_2 and CO_2 were removed from the systems by bubbling. N_2 previously scrubbed through an alkaline pyrogallol solution. During the experiments, TiO_2 particles were kept in suspension using a magnetic stirrer and a teflon-coated magnetic bar; to break aggregates, the suspensions were briefly ultrasonicated using a titanium probe. Cellulose nitrate membranes with a pore size of 0.20 μm were used for filtration.

The electrophoretic mobilities of P-25 TiO_2 particles suspended in 10^{-2} mol dm^{-3} KCl solutions were measured at 298.0 ± 0.2 K as a function of pH and catechol concentration in a Mark II Rank Brothers apparatus using a thermostated cylindrical microelectrophoresis cell. Before the measurements, the suspensions were left standing overnight under an O_2–CO_2-free atmosphere.

RESULTS

A key parameter in the description of ionic adsorption is N_S, the number of available OH surface groups, which determines the monolayer (maximum) coverage. Results from the set of KOH adsorption experiments carried out to quantify N_S are collected in Table 1. These data were fitted to a linearized Langmuir adsorption isotherm, e.g.,

$$\frac{\partial([OH^-]/\Gamma_{OH^-})}{\partial[OH^-]} = \frac{1}{N_S} = \text{const}, \qquad [1]$$

from which $N_S = 2.97 \times 10^{-6}$ mol m^{-2} (or 1.79 sites nm^{-2}) was obtained; note that under the present conditions $(\Gamma_{OH^-} - \Gamma_{H^+}) \approx \Gamma_{OH^-}$. This figure is in close agreement with the fluoride exchange capacity (1.7 sites nm^{-2}) measured for P-25 TiO_2 at pH 7.8 (34) and the maximum attainable acetate

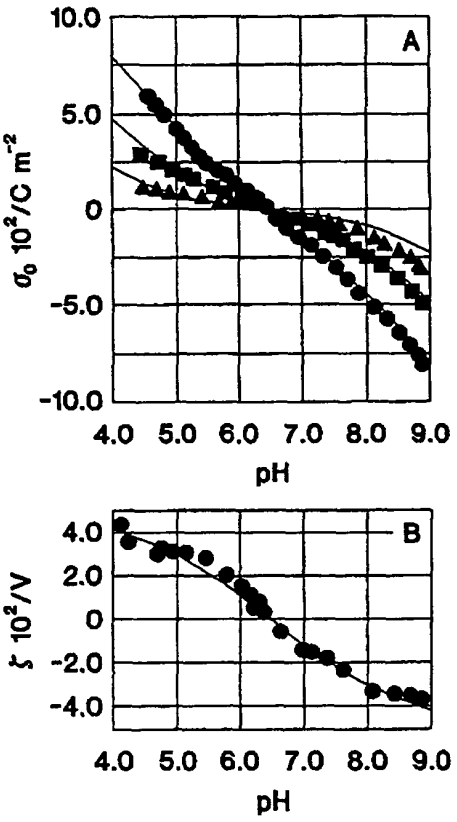

FIG. 1. pH dependence of the surface charge density (A) and ζ potential (B) of TiO_2 (anatase) particles immersed in KCl solutions: (●) 0.1 mol dm^{-3}; (■) 0.01 mol dm^{-3}; (▲) 0.001 mol dm^{-3}; data points in (B) correspond to 0.01 mol dm^{-3} KCl; T = 298 K; solid lines are model calculations (see text).

adsorption density (2.0 sites nm^{-2}) (32); in both cases, a one to one ligand exchange stoichiometry may be assumed. The reported value of N_S also agrees well with those (ca. 2.4 sites nm^{-2}) derived by Boehm (32, 35) and by van Veen *et al.* (34) from hydroxide adsorption experiments carried out under conditions similar to those of the present work.

At higher hydroxide concentrations (ca. 0.1 mol dm^{-3}), Boehm (32, 35) and van Veen *et al.* (34) observed higher OH^- consumptions, from which they derived larger N_S values (in the order 4.4–5.7 sites nm^{-2}); as a possible explanation, the existence of OH surface groups with markedly different acidic behaviors was postulated. However, the measured density of chemisorbed water is 2.3 H_2O molecules nm^{-2} (36). Thus, 4.6 sites nm^{-2} would require the ionization of *all* protons derived from chemisorbed water. It has been noted previously (8) that nondissociatively coordinated water molecules can behave only as monoprotic acids. Moreover, it has been shown that dissociative chemisorption of H_2O on TiO_2 produces only *one* acidic OH group (22–24), as further discussed below. Therefore, it seems plausible that the increased consumption of base at the higher hydroxide concentrations may reflect a nucleophilic attack of OH^- on titanium sites. In fact, participation of OH^- ions in the rate determining step of Ti(IV) dissolution from TiO_2 films in alkaline media has already been diagnosed (37).

The interfacial properties of P-25 TiO_2 immersed in indifferent electrolyte aqueous solutions is presented in Fig. 1. Figure 1A depicts proton adsorption data as a function of pH and electrolyte concentration; these data are expressed as surface charge density values, i.e., $\sigma_0 = F(\Gamma_{H^+} - \Gamma_{OH^-})$. Figure 1B shows the pH dependence of the electrokinetic potential (ζ) of P-25 TiO_2 suspended in 10^{-2} mol dm^{-3} KCl; ζ potentials were derived from experimental electrophoretic mobility data following the procedure proposed by O'Brien and White (38). The point of zero charge (pH_0 = 6.50 ± 0.05), which coincides with the isoelectric point (iep), is in excellent agreement with previously reported values (39–47); σ_0 and ζ values are also in the range of former data.

Catechol adsorption isotherms at three fixed pH values are presented in Fig. 2. Within the pH range 3.6 ≤ pH ≤ 6.0, the surface excess is almost independent of pH and presents a Langmuirian dependence with the concentration of free catechol; the Langmuir parameters are K_L = 8.2 × 10^3 mol^{-1} dm^3 and Γ_{max} = 1.25 × 10^{-6} mol m^{-2}. These values are in good concordance with those reported by Moser *et al.* (48) for the adsorption of aromatic acids from hydroalcoholic solutions onto P-25 TiO_2. While only two parameters are needed to describe the adsorption isotherms depicted in Fig. 2, the Langmuirian constants describing ionic adsorption are necessarily conditional; indeed, they may be pH dependent. In fact, the affinity of catechol for the TiO_2 surface decreases markedly at pH values larger than ca. 8.5. This is illustrated by Fig. 3, in which adsorption data ob-

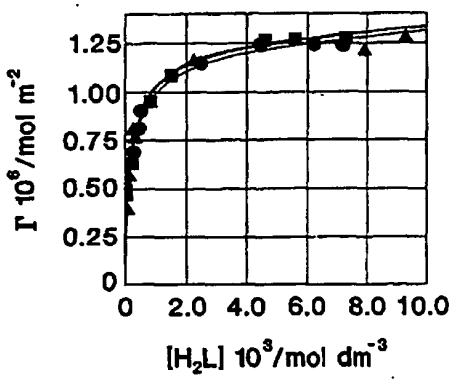

FIG. 2. Catechol adsorption isotherms for different pH values: (●) 3.65; (■) 4.25; (▲) 6.00; no added background electrolyte; T = 298 K; symbols are experimental data points; solid lines are model calculations (see text).

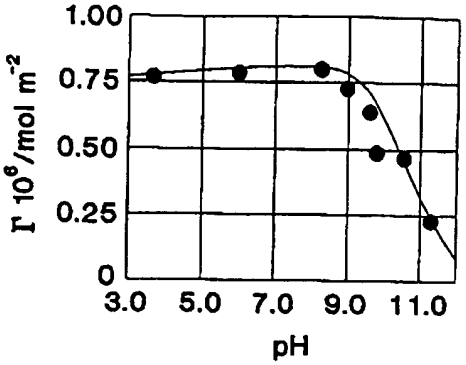

FIG. 3. Catechol surface excess as a function of pH. Total catechol concentration: 0.001 mol dm^{-3}; available TiO_2 surface area: 822.4 m^2 dm^{-3}; no added background electrolyte; T = 298 K; symbols are experimental data points; the solid line corresponds to model calculations (see text).

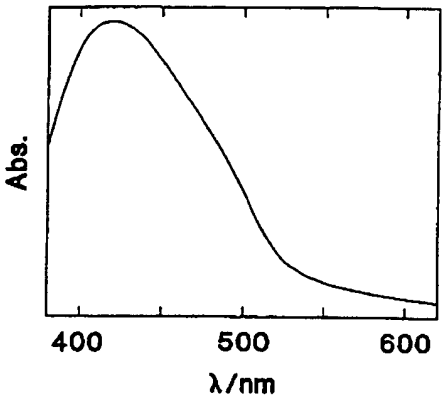

FIG. 5. Differential diffuse reflectance spectrum of surface titanium–catecholate complexes; in arbitrary absorbance units.

tained from experiments carried out at a constant total catechol concentration and at a fixed surface to volume ratio are plotted as a function of pH; note that Γ values presented in the form of Fig. 3 are sensitive to the experimental conditions, e.g., they depend on the selected surface to volume ratio.

Adsorption of catechol produces an excess of negative surface charge, thus the iep of TiO_2 particles moves to lower pH values (Fig. 4); at pH values apart from iep, however, ζ-potential values are only slightly sensitive to catechol concentration. This effect is characteristic of anionic adsorption, and indicates, as already diagnosed for the Fe_3O_4/H_3BO_3 and ZrO_2/H_3BO_3 systems (15), that surface complexation enhances the acidity of catechol. Quasi-equivalent coadsorption of protons (49), which is responsible for the insensitivity of catechol surface excess toward pH in the range 3.6–8.5 (Fig. 3), does not suffice to counterbalance the build up of negative charge that causes the observed shift.

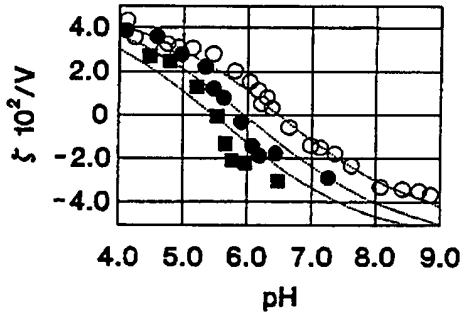

FIG. 4. The influence of catechol adsorption on ζ potential vs pH profiles; catechol equilibrium concentration: (■) 5 × 10^{-3} mol dm^{-3}; (●) 5 × 10^{-4} mol dm^{-3}; (○) in the absence of catechol; [KCl] = 0.01 mol dm^{-3}; T = 298 K; symbols are experimental data points; dotted lines are model calculations (see text).

Complexation of surface titanium ions by catechol is demonstrated by the changes in the UV–visible diffuse reflectance spectrum of TiO_2. The spectrum of TiO_2 displays the characteristic absorption edge at λ ≈ 400 nm, but, in the presence of adsorbed catechol, it presents a broad shoulder at ca. 440 nm and a tail that extends to about 700 nm; the latter resembles the absorption spectrum of the colloidal-TiO_2/catechol system reported by Moser *et al.* (48). The difference spectrum, which is presented in Fig. 5, shows a band centered at 420 nm that can be assigned to the intramolecular ligand to metal charge transfer transition within the surface titanium(IV)–catecholate complexes. This band is 30 nm red-shifted as compared to that appearing in the absorption spectrum of aqueous $Ti(cat)_3^{2-}$ complexes (λ_{max} = 389 nm) (27). Even though such shifts seem to be common when comparing the spectra of "analogous" aqueous and surface complexes (50), a conclusive explanation of the observed differences cannot yet be forwarded; differences in the coordination environments of surface and aqueous Ti(IV) ions, and coupling between the electronic levels of bulk oxide and surface complexes might, in principle, be invoked.

DISCUSSION

The Surface Site Density

The use of multi-site complexation models (22–24) requires the identification of the types of OH surface groups that determine the colloid chemistry of the oxide sample. Rigorously, such a task implies the knowledge of the actual crystal faces composing the particle habit. This is not usually the case. In principle, equilibrium crystal shape may be assumed, although particles of nano-crystalline powders, such as the P-25 TiO_2, may expose different crystal faces, including the less stable ones. Keeping this drawback in mind, we will assume, for simplicity, that the behavior of the TiO_2

(anatase)/solution interface is dominated by the properties of $\equiv TiOH^{1/3-}$ and $\equiv OH^{1/3+}$ surface groups that are created upon hydroxylation of freshly cleaved (001) and (011) surfaces (32, 33).

The acid–base character of these sites is represented by two surface equilibria:

$$\equiv TiOH_2^{2/3+} \rightleftharpoons \equiv TiOH^{1/3-} + H^+; \quad K_A^{int} \quad [2]$$

$$\equiv O^{2/3-} + H^+ \rightleftharpoons \equiv OH^{1/3+}; \quad K_B^{int}. \quad [3]$$

These equations emphasize the Brønsted acidic nature of $\equiv TiOH_2^{2/3+}$ (A sites) and the basic character of $\equiv O^{2/3-}$ (B sites). K_A^{int} and K_B^{int}, the intrinsic (potential independent) surface equilibrium constants, are given by

$$K_A^{int} = \frac{\{\equiv TiOH^{1/3-}\}[H^+]}{\{\equiv TiOH_2^{2/3+}\}} \exp(-F\psi_0/RT) \quad [4]$$

$$K_B^{int} = \frac{\{\equiv OH^{1/3+}\}}{\{\equiv O^{2/3-}\}[H^+]} \exp(F\psi_0/RT), \quad [5]$$

where { } denotes surface concentration, which will be expressed in mol m^{-2}. ψ_0 is the surface potential.

Equations [2] and [3] also stress that dissociatively chemisorbed water behaves as a monoprotic acid; deprotonation of $\equiv TiOH^{1/3-}$, if possible, may only occur in extremely alkaline media (23, 24). Thus, provided that electrostatic effects are neglected, the maximum number of titrable surface protons, N_S = 1.79 OH nm^{-2} (or 2.97 × 10^{-6} mol m^{-2}), must represent the total density of A sites. The mass balance for A sites at any pH is therefore

$$N_A = N_S = \{\equiv TiOH_2^{2/3+}\} + \{\equiv TiOH^{1/3-}\}. \quad [6]$$

The electroneutrality condition in the chargeless dehydrated bare surface requires that N_S must also equal the total density of B sites. Thus, the mass balance for B sites is

$$N_B = N_S = \{\equiv O^{2/3-}\} + \{\equiv OH^{1/3+}\}. \quad [7]$$

These simple ideas are essential to avoid the prediction of unrealistic monolayer coverages.

The TiO_2/Indifferent Electrolyte Solution Interface

Before discussing the chemisorption of catechol at the TiO_2 surface in terms of the multisite surface complexation model, a brief description of the TiO_2/indifferent electrolyte solution interface will be presented. In principle, the distribution of surface sites, hence the charging behavior of the TiO_2 surface, could be predicted if an independent expression relating ψ_0 and pH was available. Unfortunately, such an expression is lacking (51).[2] Nevertheless, the surface speciation can be calculated on the basis of a suitable electrical double layer (EDL) model by solving the set of equations that describes the charge and potential distribution across the interface. This set, which is implicitly based on the Gouy–Chapman–Stern–Grahame (GCSG) structure of the interface, is presented in Table 2. Although simpler EDL models (e.g., the constant capacitance model) can accurately describe the charging behavior of metal oxide surfaces (52), those based on the GCSG structure account better for electrokinetic potentials (7, 15).

To solve the set of equations presented in Table 2 the values of K_A^{int}, K_B^{int}, ϕ_{K^+}, ϕ_{Cl^-}, C_1, and C_2 are required; as discussed before, N_A and N_B are related to N_S which was assessed experimentally. The actual number of unknown parameters is however less, for the surface equilibrium constants are related through

$$pH_0 = \frac{1}{2}(\log K_B^{int} - \log K_A^{int}), \quad [16]$$

and equivalent specific adsorption of background electrolyte ions requires

$$\phi_{K^+} = \phi_{Cl^-}. \quad [17]$$

Dissociative chemisorption of water imposes a further constraint (cf. Eqs. [2] and [3]):

$$K_A^{int} \geq 1/K_B^{int}. \quad [18]$$

In the single-site description of metal oxide surfaces, all model parameters, with the exception of C_2, can be determined through the appropriate treatment of σ_0 vs pH and N_S data (9–14, 53, 54). In the present description of the P-25 TiO_2 surface, however, linearization of σ_0 vs pH is not possible, and unknown model parameters must be derived from the best fit to the data sets presented in Fig. 1; note that, in modeling σ_0 vs pH and ζ vs pH data, the identity, $\zeta = \psi_\delta$, is assumed to be valid. Nonlinear least-squares fitting was performed with the aid of a BASIC program written by the authors. Since capacity values must be independent of the actual description of the surface sites, previously reported values of C_1 and C_2 were used to reduce the number of

[2] Notice that a Nernstian pH dependence of ψ_0 is incompatible with any surface site model (see, for instance, Ref. (51)); if ψ_0 were a Nernstian function of pH, the ratios $\{\equiv TiOH_2^{2/3+}\}/\{\equiv TiOH^{1/3-}\}$ and $\{\equiv OH^{1/3+}\}/\{\equiv O^{2/3-}\}$ would be constant and independent of pH, viz. σ_0 would be invariant (cf. Eqs. [9]–[11]).

TABLE 2
Equations Describing the TiO_2/Indifferent Electrolyte Solution Interface According to the GCSG Structure of the Interfacial Region

Surface mass balance	$N_A = N_S = \{\equiv TiOH_2^{2/3+}\} + \{\equiv TiOH^{1/3-}\}$	[6]
	$N_B = N_S = \{\equiv O^{2/3-}\} + \{\equiv OH^{1/3+}\}$	[7]
Electroneutrality	$\sigma_0 + \sigma_\beta + \sigma_\delta = 0$	[8]
Surface charge density	$\sigma_0 = \sigma_0^+ - \sigma_0^-$	[9]
	$\sigma_0^+ = F\{\frac{2}{3}\{\equiv TiOH_2^{2/3+}\} + \frac{1}{3}\{\equiv OH^{1/3+}\}\}$	[10]
	$\sigma_0^- = F\{\frac{2}{3}\{\equiv O^{2/3-}\} + \frac{1}{3}\{\equiv TiOH^{1/3-}\}\}$	[11]
Countercharge at the β plane[a]	$\sigma_\beta = \frac{\sigma_0^- K_{K^+}[K^+]\exp(-F\psi_\beta/RT)}{1 + K_{K^+}[K^+]\exp(-F\psi_\beta/RT)} - \frac{\sigma_0^+ K_{Cl^-}[Cl^-]\exp(F\psi_\beta/RT)}{1 + K_{Cl^-}[Cl^-]\exp(F\psi_\beta/RT)}$	[12]
Countercharge at the δ plane[b]	$\sigma_\delta = 0.1174\, I^{1/2} \sinh(-F\psi_\delta/2RT)$	[13]
Charge-potential relationships	$\psi_0 - \psi_\beta = \sigma_0/C_1$	[14]
	$\psi_\beta - \psi_\delta = -\sigma_\delta/C_2$	[15]

[a] The constants K_{K^+} and K_{Cl^-} are related to the specific adsorption potentials (ϕ_i) through K_i (mol^{-1} dm^3) = $0.018 \exp(-\phi_i/RT)$.
[b] For aqueous solutions at 298 K; σ_δ is given in C m^{-2}; I is the ionic strength in mole dm^{-3}.

parameters that require optimization.[3] The model parameters that best describe the P-25 TiO_2/indifferent electrolyte solution interface are listed in Table 3. The agreement between model calculations and experimental data is noteworthy (see Fig. 1).

The calculated distribution of surface sites is depicted in Fig. 6 as a function of pH and ionic strength. As imposed by the constraint [18], the OH surface groups with the smallest charge number prevail. However, as the ionic strength increases, the fractions of $\equiv TiOH_2^{2/3+}$ and $\equiv O^{2/3-}$ become increasingly important; notice that the surface speciation at the point of zero charge is insensitive to electrolyte concentration.

TABLE 3
Model Parameters Describing the P-25 TiO_2/Indifferent Electrolyte Solution Interface

N_s (nm^{-2})	log K_A^{int}	log K_B^{int}	ϕ_{K^+}/RT	ϕ_{Cl^-}/RT	C_1 (F m^{-2})	C_2 (F m^{-2})
1.79	−5.38[a]	7.60[a]	−4.36[a]	−4.36[a]	1.40[b]	0.23[c]

[a] Obtained by fitting σ_0 vs pH and ζ vs pH data under the constraints imposed by Eqs. [16]–[18].
[b] Taken from Refs. (28, 29).
[c] Taken from Ref. (41).

[3] In principle, K_A^{int} and K_B^{int} can also be estimated independently from the correlation found by Hiemstra *et al.* (22). However, the estimated values predict a pH_0 that would range between 5.8 and 4.2, depending on the exposed crystal face. We have therefore chosen to leave K_A^{int} (or K_B^{int}) as an adjustable parameter.

Complexation of Surface Titanium Ions by Catechol

The analogy between the UV–visible spectra of Ti(IV)–catecholate aqueous complexes reported by Borgias *et al.* (27) and that shown in Fig. 5 is another example of the correspondence between surface and solution chemistry. Adsorbed catecholate anions bind surface titanium ions in a process that involves the substitution of surface coordinated OH^- (or water molecules). Since the surface complexation approach describes che-

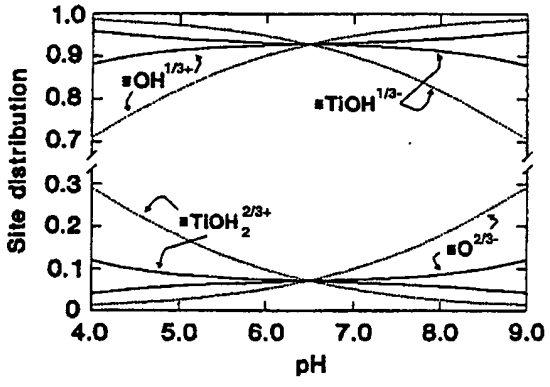

FIG. 6. Distribution of A and B surface sites in the absence of catechol; ionic strengths are 0.1 mol dm^{-3} (dotted lines) and 0.001 mol dm^{-3} (solid lines).

misorption as a fully equilibrated and totally reversible process, only the A sites (e.g., $\equiv TiOH^{1/3-}$) should be prone to reversible ligand exchange. In fact, the participation of B sites (e.g., $\equiv OH^{1/3+}$) in a ligand exchange surface reaction must be impeded, at least kinetically, by the large energetic requirement involved in the rupture of titanium-oxo bonds. Also, any ligand exchange involving B sites must be highly irreversible, because surface reconstruction (a sluggish process) should be expected to follow ligand desorption. Incidentally, a combined attack of ligands (nucleophilic attack) and protons (electrophilic attack) on metal-oxo bonds usually leads irreversibly to dissolution (6); as mentioned, this process may be involved in OH^- "adsorption" in very basic media. Therefore, the chemisorption of catechol (or other complexing anions) at the TiO_2/aqueous solution interface will be limited by the availability of A surface sites.

The information provided by the spectrum in Fig. 5 is, however, insufficient to identify the possible Ti–catecholate surface complexes, which therefore have to be inferred from the observed adsorption behavior. In principle, two surface complexation equilibria may be postulated:

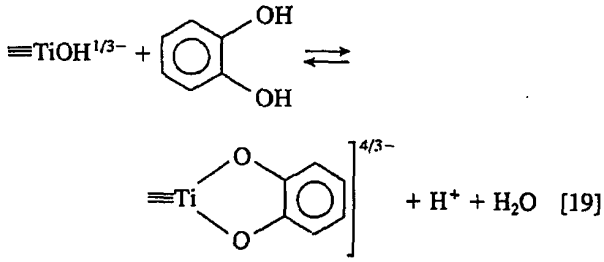

$$\equiv TiOH^{1/3-} + \text{catechol} \rightleftharpoons \equiv Ti(\text{catechol})^{4/3-} + H^+ + H_2O \quad [19]$$

(I)

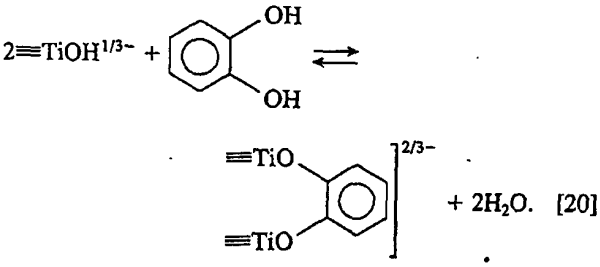

$$2{\equiv}TiOH^{1/3-} + \text{catechol} \rightleftharpoons (\equiv TiO)_2(\text{catechol})^{2/3-} + 2H_2O. \quad [20]$$

(II)

The catechol adsorption density is thus given by the sum

$$\Gamma = \{I\} + \{II\}. \quad [21]$$

Adsorption in a 1 to 1 $\equiv$Ti:catechol ratio (Eq. [19]) has already been proposed by Moser *et al.* (48). In terms of the present representation of the OH surface groups, formation of 1 to 1 surface complexes (species I) would imply that surface titanium ions adopt the uncommon hepta-coordination. On the other hand, surface titanium ions retain their normal coordination environment in species II (Eq. [20]). Thus, although the distortion of the TiO_6 octahedra in species II must increase to accommodate for the mismatch between the O–O distance in the catecholate ion and the surface Ti–Ti distance (in the most occurring (001) and (011) anatase cleavage planes, this is 3.78 Å), the formation of species II would be expected to predominate, particularly at pH values below pK_{a1} (cf. Eqs. [19] and [20]). In fact, surface equilibrium [20] accounts for both the prevailing adsorption stoichiometry (indicated by the ratio $\Gamma_{max}:N_S = 0.42$) and the noted pH dependence of the adsorption density (Figs. 2 and 3). Formation of species I is, however, essential to account for the increased negative surface charge (i.e., the shifts in iep shown in Fig. 4). Even though other adsorption modes could also be invoked (see, e.g., Refs. (12–14) and (49)), those depicted by Eqs. [19] and [20] suffice to describe our experimental results. The corresponding surface equilibrium constants are

$$K_I^{int} = \frac{\{I\}[H^+]}{\{\equiv TiOH^{1/3-}\}[H_2L]} \exp(-F\psi_0/RT) \quad [22]$$

$$K_{II}^{int} = \frac{\{II\}}{\{\equiv TiOH^{1/3-}\}^2[H_2L]}, \quad [23]$$

where H_2L denotes catechol. As is usual for surface isocoulombic reactions, $\{II\}$ does not depend on surface potential; obviously, any change in ψ_0 may influence $\{II\}$ through its effect on the coupled surface equilibria. A quadratic dependence of $\{II\}$ with the surface concentration of $\equiv TiOH^{1/3-}$ (Eq. [23]) was chosen to represent the need of finding two vicinal A sites available for the formation of a 2 to 1 surface complex. It has been suggested, however, that a linear relationship between $\{II\}$ and $\{\equiv TiOH^{1/3-}\}$ is also consistent with this requirement (55). Stumm and co-workers (13, 14) have pointed out that the most realistic value of the exponent (n) on $\{\equiv TiOH^{1/3-}\}$ in Eq. [23] must lie in the range $2 \geq n \geq 1$, and showed that a reasonable description of the stability of binuclear surface complexes can be offered by setting $n = 1$. Instead, we chose to set $n = 2$, for it allows for a consistent description of the equilibrium between species I and II, i.e.,

$$II + H_2L \rightleftharpoons 2I + 2H^+. \quad [24]$$

The same choice was made by Müller and Sigg (55) to report β_2^S, the stability constant of the $(\equiv FeOO)_2Pb$ surface complex.

The set of equations presented in Table 2 also describes the TiO_2/catechol aqueous solution interface. Equations [6]

TABLE 4
Surface Complexation Equilibria at the P-25 TiO_2/Catechol Aqueous Solution Interface

	Surface equilibrium	log K^{int}
B sites	$\equiv O^{2/3-} + H^+ \rightleftharpoons \equiv OH^{1/3+}$; K_B^{int}	7.60
A sites	$\equiv TiOH^{1/3-} + H^+ \rightleftharpoons \equiv TiOH_2^{2/3+}$; $1/K_A^{int}$	5.38
	$\equiv TiOH^{1/3-} + H_2L \rightleftharpoons \equiv TiL^{4/3-} + H^+ + H_2O$; K_I^{int} [a]	−3.00
	$2 \equiv TiOH^{1/3-} + H_2L \rightleftharpoons (\equiv Ti)_2L^{2/3-} + 2H_2O$; K_{II}^{int} [a]	3.20

[a] Eqs. [19] and [20] were rewritten for simplicity.

and [11] were appropriately modified to include the surface complexes I and II:

$$N_A = N_S = \{\equiv TiOH_2^{2/3+}\} + \{\equiv TiOH^{1/3-}\} + \{I\} + 2\{II\} \quad [6']$$

$$\sigma_0^- = F\left[\frac{2}{3}\{\equiv O^{2/3-}\} + \frac{1}{3}\{\equiv TiOH^{1/3-}\} + \frac{4}{3}\{I\} + \frac{2}{3}\{II\}\right] \quad [11']$$

The values of K_I^{int} and K_{II}^{int} that best characterize the chemisorption behavior of catechol onto P-25 TiO_2 are included in Table 4, where the surface equilibria that take place in this system are summarized. The model parameters listed in Table 3 should not be affected, in principle, by catechol adsorption.

Model calculations presented in Figs. 2 and 3 demonstrate that the multisite surface complexation model accounts excellently for the observed chemisorption behavior. The agreement between predicted and experimental ζ potentials is, however, less satisfactory (Fig. 4). Although the dependence of iep with catechol concentration is fairly well reproduced, the model underestimates the slopes $\partial\zeta/\partial$pH, particularly in the vicinity of iep. Adsorbed catechol may affect the inner structure of the electrical double layer; adsorbed ligands should alter the locus of specifically adsorbed counterions, an effect that reflects itself essentially on C_1. A suitable modification of the internal region of the interface, e.g., following the ideas introduced by Smit (56, 57), may improve the performance of the model.

Although there is no implicit relationship between the ligand adsorption density and the concentration of indifferent electrolyte, the model predicts a noticeable influence of ionic strength. This is illustrated by Fig. 7, where the contributions of species I and II to the adsorption density are plotted as a function of pH and electrolyte concentration. The marked change of $\partial\Gamma/\partial$pH (pH < pK_{a1}) is a consequence of the increased screening effect due to the swamping electrolyte; it favors protonation of $\equiv TiOH^{1/3-}$ sites at pH < pH_0 (cf. Fig. 6) and enhances the contribution of species I at pH values within pH_0 and pK_{a1}. In a thorough study of the adsorption of catechol on γ-Al_2O_3 in 0.1 mol dm^{-3} $NaClO_4$, Kummert and

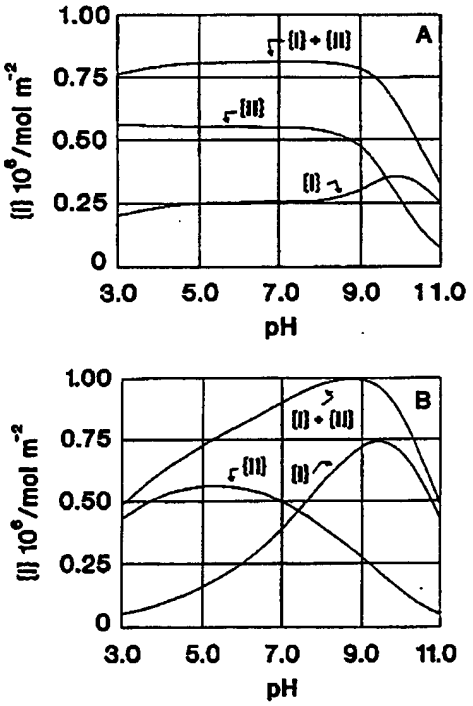

FIG. 7. The influence of ionic strength on the speciation of surface titanium–catecholate complexes: (A) no added background electrolyte; (B) in the presence of 0.1 mol dm^{-3} KCl. Total catechol concentration: 0.001 mol dm^{-3}; available TiO_2 surface area: 822.4 m^2 dm^{-3}; T = 298 K.

Stumm (13) report positive values of $\partial\Gamma/\partial$pH (pH < pK_{a1}). This is in contrast with the trend shown in Fig. 3. However, the dissimilar behaviors may be interpreted on the basis of the predicted influence of ionic strength; TiO_2 and γ-Al_2O_3 may also behave differently toward catechol adsorption due to their different complexation chemistry (note also the different values of pH_0).

Comparison with the Single-Site Approach

The outstanding ability of the multisite surface complexation model to describe the chemisorption behavior of weak acids at metal oxide/aqueous solution interfaces is largely shared by the single-site versions of the surface complexation approach. In fact, the surface equilibria depicted by Eqs. [19] and [20] are compatible with the single-site description (only a minor change in notation is required) and, if the appropriate surface equilibrium constants are used, the adsorption of catechol at the P-25 TiO_2/solution interface can also be accounted for on the basis of any suitable single-site surface complexation model.

The noticeable influence of ionic strength anticipated by the present model (Fig. 7) is also predicted by the single-site models that are based on GCSG structure of the electrical double layer (15, 58); in the latter description, the effect of indifferent electrolyte concentration is accounted for by surface ion-pairing equilibria involving charged surface complexes and coadsorbed counterions. The implications of the different EDL structures that are assumed by single-site surface complexation models had already been discussed in the literature (7, 58).[4]

Although both the single-site and the multisite surface complexation models offer an excellent description of the chemisorption of catechol at the P-25 TiO_2/aqueous solution interface, the internal coherence of all the model assumptions favors the use of the present multisite approach that does not require the use of an increased number of adjustable parameters.

ACKNOWLEDGMENTS

Partial support by Fundación Antorchas is gratefully acknowledged. The authors are members of CONICET.

REFERENCES

1. Hohl, H., Sigg, L., and Stumm, W., *in* "Particulates in Water" (M. C. Kavanaugh and J. O. Leckie, Eds.), Advances in Chemistry Series, Vol. 189, p. 1. Am. Chem. Soc., Washington, DC, 1980.
2. Blesa, M. A., Regazzoni, A. E., and Maroto, A. J. G., *Mater. Sci. Forum* **29**, 31 (1988).
3. Dzombak, D. A., and Morel, F. M. M., "Surface Complexation Modeling, Hydrous Ferric Oxide." Wiley–Interscience, New York, 1990.
4. Stumm, W., "Chemistry of the Solid–Water Interface." Wiley–Interscience, New York, 1992.
5. Stumm, W., *Colloids Surf. A* **73**, 1 (1993).
6. Blesa, M. A., Morando, P. J., and Regazzoni, A. E., "Chemical Dissolution of Metal Oxides." CRC Press, Boca Raton, FL, 1994.
7. Regazzoni, A. E., Blesa, M. A., and Maroto, A. J. G., *J. Colloid Interface Sci.* **122**, 315 (1988).
8. Blesa, M. A., Maroto, A. J. G., and Regazzoni, A. E., *J. Colloid Interface Sci.* **140**, 287 (1990).
9. Davis, J. A., James, R. O., and Leckie, J. O., *J. Colloid Interface Sci.* **63**, 408 (1978).
10. Davis, J. A., and Leckie, J. O., *J. Colloid Interface Sci.* **74**, 32 (1980).
11. James, R. O., and Parks, G. A., *in* "Surface and Colloid Science" (E. Matijević, Ed.), Vol. 12, Chap. 2. Plenum, New York, 1982.
12. Stumm, W., Kummert, R., and Sigg, L., *Croat. Chem. Acta* **53**, 291 (1980).
13. Kummert, R., and Stumm, W., *J. Colloid Interface Sci.* **75**, 373 (1980).
14. Sigg, L., and Stumm, W., *Colloids Surf.* **2**, 101 (1981).
15. Blesa, M. A., Maroto, A. J. G., and Regazzoni, A. E., *J. Colloid Interface Sci.* **99**, 32 (1984).
16. Tejedor-Tejedor, M. I., and Anderson, M. A., *Langmuir* **2**, 203 (1986).
17. Zeltner, W. A., and Anderson, M. A., *Langmuir* **4**, 469 (1988).
18. Tunesi, S., and Anderson, M. A., *Langmuir* **8**, 487 (1992).
19. Hayes, K. F., Roe, A. L., Brown, G. E., Jr., Hodgson, K. O., Leckie, J. O., and Parks, G. A., *Science* **238**, 783 (1987).
20. Mulcahy, F. M., Fay, M. J., Proctor, A., Houalla, M., and Hercules, D. M., *J. Catal.* **124**, 231 (1990).
21. Pulfer, K., Schindler, P. W., Westall, J. C., and Grauer, R., *J. Colloid Interface Sci.* **101**, 554 (1984).
22. Hiemstra, T., van Riemsdijk, W. H., and Bolt, G. H., *J. Colloid Interface Sci.* **133**, 91 (1989).
23. Hiemstra, T., de Wit, J. C. M., and van Riemsdijk, W. H., *J. Colloid Interface Sci.* **133**, 105 (1989).
24. Hiemstra, T., and van Riemsdijk, W. H., *Colloids Surf.* **59**, 7 (1991).
25. Sommer, L., *Collect. Czech. Chem. Commun.* **28**, 2102 (1963).
26. Martell, E. A., and Smith, R. M., "Critical Stability Constants" Vol. 3. Plenum, New York, 1976.
27. Borgias, B. A., Cooper, S. R., Koh, Y. B., and Raymond, K. N., *Inorg. Chem.* **23**, 1009 (1984).
28. Yates, D. E., Levine, S., and Healy, T. W., *J. Chem. Soc., Faraday Trans. 1* **70**, 1807 (1974).
29. Yates, D. E., Ph.D. Thesis, University of Melbourne, Australia, 1975.
30. Jones, P., and Hockey, J. A., *Trans. Faraday Soc.* **67**, 2679 (1971).
31. Jackson, P., and Parfitt, G. D., *Trans. Faraday Soc.* **67**, 2469 (1971).
32. Boehm, H. P., *Disc. Faraday Soc.* **52**, 264 (1971).
33. Dorémieux-Morin, C., Enriquez, M. A., Sanz, J., and Fraissard, J., *J. Colloid Interface Sci.* **95**, 502 (1983).
34. van Veen, J. A. R., Veltmaat, F. T. G., and Jonkers, G., *J. Chem. Soc., Chem. Commun.* 1656 (1985).
35. Herrmann, M., and Boehm, H. P., *Z. Anorg. Chem.* **368**, 73 (1969).
36. Boehm, H. P., and Herrmann, M., *Z. Anorg. Chem.* **352**, 156 (1967).
37. Allard, K. D., and Heusler, K. E., *J. Electroanal. Chem.* **77**, 35 (1977).
38. O'Brien, R. W., and White, L. R., *J. Chem. Soc., Faraday Trans. 2* **74**, 1607 (1978).
39. Schindler, P. W., and Gamsjäger, H., *Disc. Faraday Soc.* **52**, 286 (1971).

[4] It is important to stress that these implications can only be assessed properly through the detailed study of the influence of ionic strength on anion chemisorption. In view of the scarcity of data, we have undertaken this task which will be reported in a future communication.

40. Schindler, P. W., and Gamsjäger, H., *Kolloid Z. Z. Polym.* **250,** 759 (1972).
41. Foissy, A., M'Pandou, A., Lamarche, J. M., and Jaffrezic-Renault, N., *Colloids Surf.* **5,** 363 (1982).
42. M'Pandou, A., and Siffert, B., *J. Colloid Interface Sci.* **102,** 138 (1984).
43. Furlong, D. N., Wells, D., and Sasse, W. H. F., *J. Phys. Chem.* **89,** 626 (1985).
44. Janssen, M. J. G., and Stein, H. N., *J. Colloid Interface Sci.* **109,** 508 (1986).
45. Girod, G., Lamarche, J. M., and Foissy, A., *J. Colloid Interface Sci.* **121,** 265 (1988).
46. Miller, N. P., and Berg, J. C., *Colloids Surf.* **59,** 119 (1991).
47. Avena, M. J., Ph.D. Thesis, Universidad Nacional de Córdoba, Argentina, 1993.
48. Moser, J., Punchihewa, S., Infelta, P. P., and Grätzel, M., *Langmuir* **7,** 3012 (1991).
49. Borghi, E. B., Morando, P. J., and Blesa, M. A., *Langmuir* **7,** 1652 (1991).
50. Regazzoni, A. E., and Blesa, M. A., *Langmuir* **7,** 473 (1991).
51. Blesa, M. A., and Kallay, N., *Adv. Colloid Interface Sci.* **28,** 111 (1988).
52. Westall, J. C., and Hohl, H., *Adv. Colloid Interface Sci.* **12,** 265 (1980).
53. Smit, W., and Holten, C. L. M., *J. Colloid Interface Sci.* **78,** 1 (1980).
54. Regazzoni, A. E., Ph.D. Thesis, Universidad Nacional de Tucumán, Argentina, 1984.
55. Müller, B., and Sigg, L., *J. Colloid Interface Sci.* **148,** 517 (1992).
56. Smit, W., *J. Electrochem. Soc.* **132,** 2172 (1985).
57. Smit, W., *J. Colloid Interface Sci.* **109,** 295 (1986).
58. Hayes, K. F., Papelis, C., and Leckie, J. O., *J. Colloid Interface Sci.* **125,** 717 (1988).